Cite This: Org. Process Res. Dev. 2020, 24, 85–95

pubs.acs.org/OPRD

Third-Generation Method for High-Throughput Quantification of Trace Palladium by Color or Fluorescence

Lydia Lukomski, Ivanna Pohorilets, and Kazunori Koide*

Department of Chemistry, University of Pittsburgh, 219 Parkman Avenue, Pittsburgh, Pennsylvania 15260, United States

Supporting Information

ABSTRACT: Chemists frequently encounter problems associated with trace palladium in synthetic samples because palladium is widely used in synthetic organic chemistry. We previously reported a colorimetric method for trace palladium quantification, the only high-throughput method implemented in the pharmaceutical industry. However, slight changes from the published reaction conditions have caused reproducibility problems, with little understanding of underlying molecular mechanisms. In the current study, we took a combinatorial approach to investigate the method and found that excess NaOH was a culprit for the lack of reproducibility. We changed the reaction conditions and procedure accordingly, which substantially improved reproducibility. The reaction under current conditions followed Michaelis-Menten kinetics, allowing for predicting reaction rates on the basis of the substrate concentrations. The current method showed 57 and 72% average error, respectively, when drugs spiked with known amounts of palladium and synthetic samples with unknown amounts of palladium were analyzed. The trend of palladium concentrations determined by the current method boded well with actual palladium concentrations.

KEYWORDS: allylic compound, fluorescent probe, high-throughput screening, palladium, trace analysis, UV-vis spectroscopy

■ INTRODUCTION

To comply with government's regulations (e.g., USP (232) in the United States),1 the pharmaceutical industry must ensure that heavy metals are below their toxic levels in active pharmaceutical ingredients (APIs). Among heavy metals, palladium is the most frequently used transition metal in chemical synthesis² and must be below 10 ppm in APIs, according to USP (232). Therefore, process chemists must develop a specific and highly efficient palladium-scavenging protocol for each API to meet the safety regulation. This is accomplished through screenings of dozens of potential workup protocols and scavengers, among other purification techniques.³⁻¹⁰ This process generates several dozens of samples in which to quantify palladium. Meanwhile, new scavengers continue to emerge, 7,11-15 adding options to explore.

As the Procedure and Detection Technique section of USP(233) states, trace metal analysis has been performed using inductively coupled plasma mass spectrometry (ICP-MS). 16-20 Unfortunately, ICP-MS is a highly specialized, costly method for analyzing palladium. The instrument is large and expensive, requires highly skilled experimentalists, a long calibration time upon starting, and expensive materials to maintain operation. Additionally, ICP-MS often becomes the bottle neck of the entire API purification process because scavenger screenings are high-throughput, while ICP-MS is low throughput, thus slowing the process. It should be noted that neutron activation analysis has been recently employed for palladium quantification.²¹

As such, high-throughput platforms are needed to streamline the API production process. A grand challenge is to shift from the established, but time-consuming, paradigm to highthroughput experimentation, even at the expense of accuracy to some extent.²² Fluorometric and colorimetric methods are high-throughput and easy to master. Moreover, fluorescence and/or UV-vis plate readers are inexpensive, robust, and do not require calibration. Due to the ease of use and portability of fluorometers, a colorimetric or fluorometric method can be employed on site (i.e., in the laboratory where APIs are purified), eliminating the need to transport synthetic samples.

We developed a high-throughput method for quantifying trace palladium in APIs by fluorescence or color (Scheme 1).^{23,24} In this method, resorufin allyl ether (RAE) undergoes palladium-catalyzed allylic C-O bond cleavage (Tsuji-Trost type reaction) to produce fluorescent, magenta resorufin in its anion form. The correlation between the resorufin concentration and fluorescence signals with our instrument (see the experimental procedure section for detail) is shown in Figure 1. The reaction is accelerated by tri(2-furyl)phosphine (TFP) and sodium borohydride (NaBH₄). The roles of TFP are 2fold: first, it binds to palladium to form catalytically active species; 25-27 second, it acts as a nucleophile. 28 The reaction autonomously stalls due to the air-oxidation of palladium(0) when NaBH₄ is used up and can be restarted upon the addition of more NaBH₄, broadening the dynamic range with respect to palladium concentration. This is convenient when the signal intensity continuously increases over time because it is difficult to start and analyze dozens of reactions in wells. In other words, autonomous stalling provides unorthodox, timeindependent data after a certain period for the catalysisbased method. This method has been implemented in the multiwell-format²³ and in flow chemistry in the pharmaceutical industry.²⁴ Others have used similar O-deallylation reactions with different fluorophores or prodrugs as analytical 29 or biological tools. $^{30-38}$

Received: November 1, 2019 Published: December 10, 2019



85

Scheme 1. Pd-Catalyzed Deallylation of Resorufin Allyl Ether

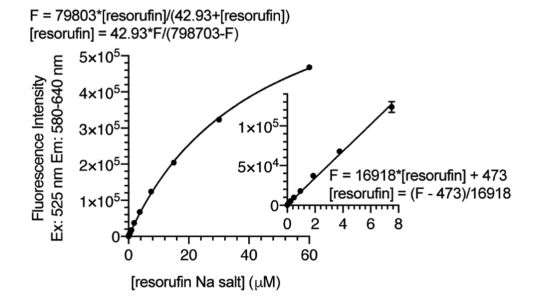


Figure 1. Standard curve for resorufin sodium salt with 180 μ M TFP and 200 mM NH₄OAc in 6:17:77 v/v dimethyl sulfoxide (DMSO)/H₂O/EtOH. F = fluorescence intensity (arbitrary unit) using a filter for 525 nm excitation and 580–640 nm emission on a plate reader.

DMSO was used in our previous and current methods because it dissolves most APIs and thus is frequently used to prepare stock solutions for trace metal analysis. However, excess DMSO was avoided because it decelerated the deallylation reaction in the previous system, although the upper limit of the DMSO amount was not specified.²³ chose EtOH as the majority of the assay mixture to accommodate both aqueous and organic layers during the extraction process after a palladium-catalyzed synthetic reaction is employed. A small fraction of water is necessary to dissolve NaBH₄. Resorufin is strongly fluorescent only above pH 4.8,³⁹ necessitating buffering or basifying the assay solutions. Although phosphate ions accelerate the palladiumcatalyzed allylic C-O bond cleavage, 29 phosphate reagents are not sufficiently soluble when the assay solution contained only a small fraction of water. Instead, NH₄OAc was chosen to neutralize acids that may be part of palladium-contaminated organic polymers after sample digestion with acid.²²

The concentrations for most components were optimized by evaluating one component at a time.²³ Recently, our group began applying the technology to real-world samples. These studies required perturbations of components' concentrations

and the order of addition of chemicals, which afforded nonreproducible results. These problems made us realize that the reaction conditions might not be optimal because some reagents react with each other, necessitating the simultaneous perturbation of multiple parameters. Therefore, we decided to develop a more robust method while investigating how the relative concentrations of reagents impact reproducibility and sensitivity. This work has resulted in a more sensitive method for quantifying palladium. It has also provided a blueprint for reproducibility, and no experiments failed during this study after the blueprint emerged.

RESULT

Problems with the Previous Method. Our original aims were to improve the sensitivity of the previous colorimetric method and to improve the reproducibility. Our previous conditions are summarized in entry 1 (Table 1). At the outset of this study, we performed experiments with lower concentrations of NH4OAc because this salt is difficult to dissolve in EtOH. Specifically, the reactions were performed under the reaction conditions shown in entry 2.1 (Figure 2a, circles); although the signals were weak, a linear correlation between the palladium concentration and fluorescence signal (excitation 525 nm, emission 580-640 nm) was observed. After 16 min, the reactions autonomously stalled. Because the color change was not visibly obvious, as shown in the photograph, we restarted the catalysis with additional NaBH₄ (stop-and-go). As expected from our previous work, 23 both the color and fluorescence signals intensified (entry 2.2). The second addition of NaBH₄ further increased both the color and fluorescence intensities (entry 2.3). However, in the 0-0.8 nM palladium range (the first three columns), the solutions changed from yellow to purple, making it difficult to visibly distinguish the magenta color from the purple color. We were also aware that too many parameters, such as time and the concentrations of NaBH₄, NaOH, and H₂O, varied in entries 2.1, 2.2, and 2.3. When the NaBH₄ concentration was 50 mM

Table 1. All of the Reactions were Performed at 24 °C with 0-250 nM PdCl₂

entry	RAE (μM)	TFP (μM)	$NaBH_4\ (mM)$	NaOH (mM)	NH ₄ OAc (mM)	DMSO (% v/v)	H_2O (% v/v)	EtOH (% v/v)	time (min)
1	29	200	2-75	235	626	7	12	81	60
2.1	30	200	10	50	300	6	12	82	16
2.2	27	181	45	405	272	5.5	20	74.5	16
2.3	23	167	75	700	250	5	26	69	16
3	30	200	50	500	300	6.5	12	81.5	16
4	30	180	50	20-420	250	6	20	74	16
5	30	180	50	70	0-375	6	9	85	16
6	30	180	50	120	0-375	6	10	84	16

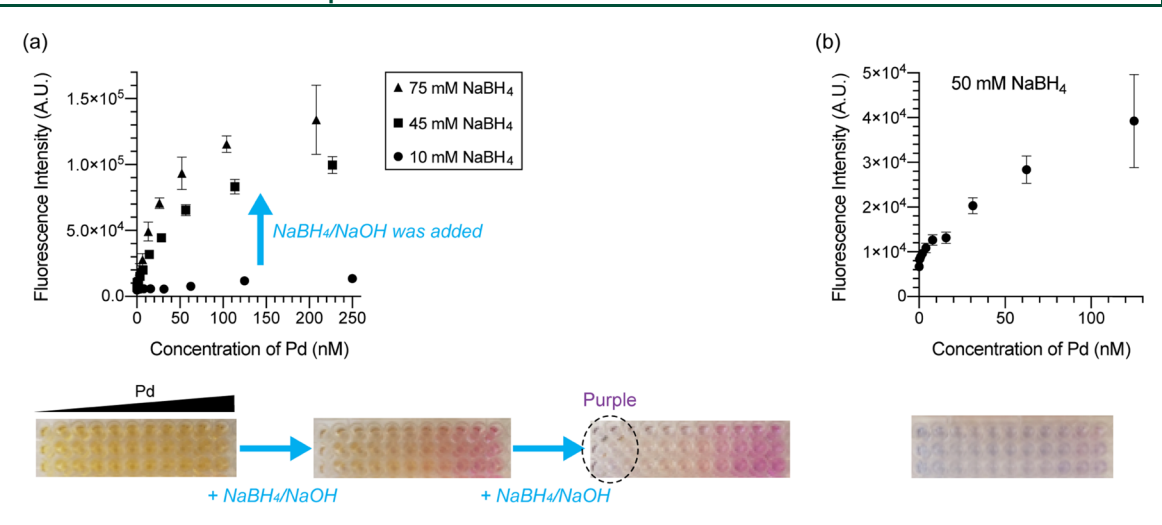


Figure 2. (a) Sequential additions of NaBH₄. (b) Starting with a high concentration of NaBH₄. Fluorescence values refer to emission signals in the 580–640 nm range with excitation at 525 nm.

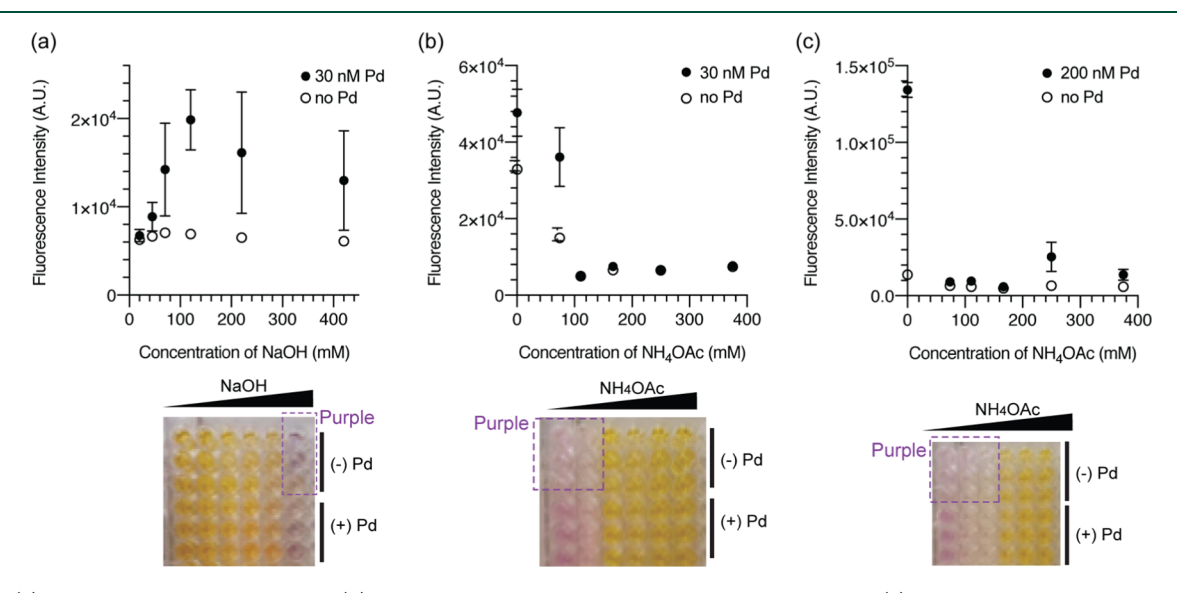


Figure 3. (a) Effect of NaOH concentration. (b) Effect of NH₄OAc concentration with 70 mM NaOH. (c) Effect of NH₄OAc concentration with 120 mM NaOH. Fluorescence values refer to emission signals in the 580–640 nm range with excitation at 525 nm.

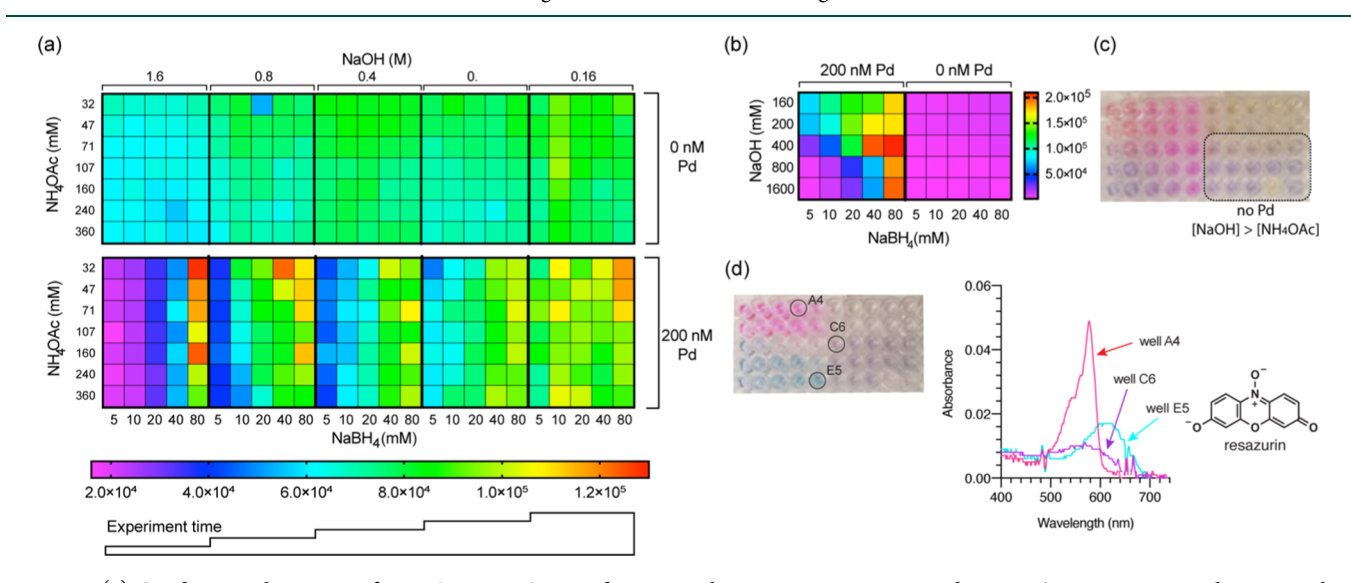


Figure 4. (a) Combinatorial screening for NaOH, NH₄OAc, and NaBH₄. Fluorescence intensities in the 580–640 nm range are shown in color. (b) and (c) Combinatorial screening for NaOH and NaBH₄ with 200 mM NH₄OAc. (c) Photograph of (b). (d) 24 h after the screening in (b).

Organic Process Research & Development

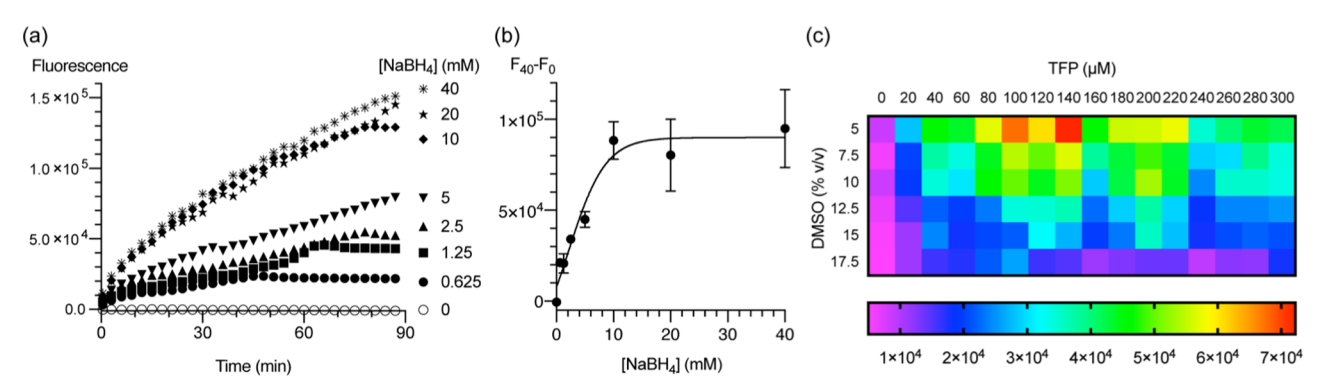


Figure 5. [NaBH₄]-dependent autonomous stalling. Fluorescence values refer to emission signals in the 580–640 nm range with excitation at 525 nm. Conditions: 180 μ M TFP, 30 μ M RAE, 0, 0.625, 1.25, 2.5, 5, 10, 20, or 40 mM NaBH₄, 100 mM NaOH, 200 mM NH₄OAc, 6:15:79 v/v DMSO/H₂O/EtOH, 31 nM PdCl₂, 24 °C, 87 min (read fluorescence every 3 min), n=2. (a) Time-dependence is shown. (b) [NaBH₄]-dependence is shown at the 40 min point. F_{40} – F_0 values are shown as the y-axis (F_{40} or F_0 = fluorescence signal at t=40 or 0 min). (c) Reaction conditions: 0–300 μ M TFP, 30 μ M RAE, 1.0 mM NaBH₄, 100 mM NaOH, 200 mM NH₄OAc, 5–17.5:20:75–42.5 v/v DMSO/H₂O/EtOH, 30 nM Pd, 24 °C, 60 min, n=1.

from the beginning (entry 3), all of the solutions turned purple (Figure 2b).

Because the observations above were not easily interpreted, we redesigned an experiment so that only the NaOH concentration would vary (entry 4 and Figure 3a). Both the lower and higher NaOH concentrations decelerated the deallylation reaction. We initially thought that at lower NaOH concentrations, NaBH₄ degraded rapidly and thus was unable to reduce air-oxidized palladium species. At higher NaOH concentrations, once again, the reactions turned purple. If the method can tolerate only a narrow range of NaOH concentrations, this would make the method difficult to employ. As we discuss below, this was not the case.

With the tentatively optimal NaOH concentration (70 mM), we investigated the effect of the NH₄OAc concentration (entry 5 and Figure 3b). When the NH₄OAc concentration was above 100 mM, there was no difference between palladium-free solutions and 30 nM palladium solutions. When the NH₄OAc concentration was below 100 mM, 30 nM palladium solutions showed increased signals. Importantly, the lower NH₄OAc concentrations increased the background signals with no palladium and turned the solutions purple. When the NaOH concentration was increased from 70 to 120 mM (entry 6 and Figure 3c), we observed the same trend. Figure 3b,c shows that the reaction was faster when the NH₄OAc concentration was lower. However, for visual estimation of the relative palladium concentration, the palladium-independent purple color with less NH4OAc was unfavorable because the readout of this system with higher palladium concentrations is magenta color. Therefore, NH₄OAc must be at a certain concentration to prevent background signal increase.

Three components are at play: (1) NH₄OAc reacts with NaOH to form NH₃, NaOAc, and H₂O, (2) NaOH is necessary to stabilize NaBH₄ in water, and (3) NaBH₄ reacts with NH₄OAc to form NaBH₃OAc, NH₃, and H₂. At this point in this study, we realized that the traditional approach through optimizing one parameter at a time might not be the best. As such, we simultaneously titrated NH₄OAc, NaOH, and NaBH₄ using ten 96-well plates (Figure 4a). It is important to note that we started reading the 96-well plate with 1.6 M NaOH and ended with the 0.16 M NaOH plate, for which ~4 min gap between plates was inevitable. Palladium-free reaction mixtures showed stronger signals over time. Apparently, NaOH converts RAE to a purple compound in the absence of palladium. Also,

within a 96-well plate with the same NaOH concentration, higher NH₄OAc concentrations slowed the NaOH-mediated formation of a purple compound more effectively, presumably because NH₄OAc neutralizes NaOH. Because the reaction times of the plates on the right side of the figure were longer, the signals were stronger despite the lower NaOH concentrations. With 200 nM palladium, fluorescence signals were higher with more NaBH₄. Particularly, with 80 mM NaBH₄ and 1.6 M NaOH, the signals were the highest in the entire panel. However, the same panel showed the greatest sensitivity to the NaBH₄ concentration. This is undesirable for the development of robust and reproducible technology for palladium quantification because NaBH4 in aqueous solution degrades even when stabilized by NaOH, 40 and the actual NaBH₄ concentration in reaction solutions may vary in day-today operations.

It is crucial to neutralize acids stemming from palladiumcontaining solutions for reproducibility. Therefore, although lower concentrations of NH₄OAc show stronger signals, we chose 200 mM NH₄OAc. With this concentration, we performed the next round of a combinatorial assay for NaOH and NaBH₄ (Figure 4b); lower signals were observed with the combination of low NaBH4 concentration and high NaOH concentration. We also found that when the NaOH concentration was above the NH₄OAc concentration, the result depended too highly on the NaBH₄ concentration, which is undesirable for the reason we stated above. Therefore, we conclude that the NaOH concentration must be below the NH₄OAc concentration, which is also corroborated with the photograph in Figure 4c; palladium-free solutions showed a purple color when the NaOH concentration was higher than the NH₄OAc concentration.

One of the advantageous features of the stop-and-go method is that the users can analyze the data many hours later or even the next day because once the assay stalls, the signals remain the same afterward. This is not the case when the NaOH concentration is above the NH₄OAc concentration, because in the presence of palladium, the solutions turned blue (Figure 4d). The UV—vis spectrum of the solution in well E5 (200 nM PdCl₂, 1.6 M NaOH, 360 mM NH₄OAc) suggested that the blue color may be due to the formation of resazurin by the palladium-O₂ catalysis. Therefore, although these reaction conditions showed an expected signal immediately after the

assay was complete, we recommend the users not to add more NaOH than NH_4OAc .

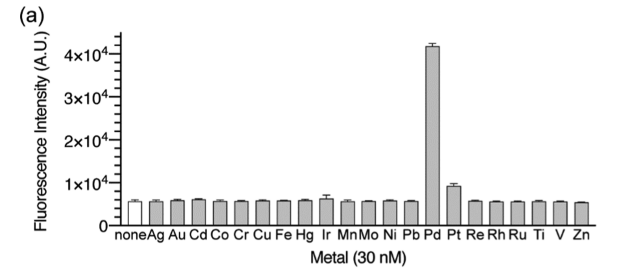
Order of Addition. For convenience, the deallylation should start as soon as the last solution is added to wells. Because NaBH₄ gradually reacts with water or NH₄OAc to become inactive, NaBH₄ must be added last. Although the palladium-catalyzed deallylation of RAE is accelerated by TFP and NaBH₄, the reaction slowly proceeds in the absence of NaBH₄ because kinetically inferior TFP can still reduce oxidized palladium species to palladium(0). Therefore, we decided that the last solution to add (starter solution) would be a mixture of TFP, NaBH₄, and NaOH. In the new order of addition, each well would be treated with (1) a mixture of RAE and NH₄OAc, (2) palladium, and (3) a mixture of TFP, NaBH₄, and NaOH in this order. This order of addition has substantially improved reproducibility throughout the remainder of this study.

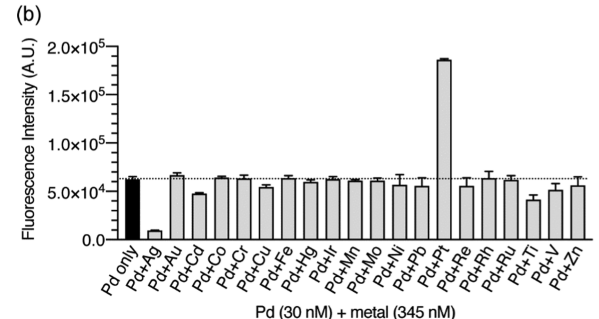
Autonomous Stalling. Next, we aimed to determine the NaBH₄ concentration range in which the deallylation autonomously stalls (Figure 5a). When the NaBH₄ concentration was \leq 2.5 mM, the reaction stalled in 45–78 min. When higher sensitivity is desired, the NaBH₄ concentration should be \geq 5 mM. Figure 5b shows that when the NaBH₄ concentration is above 10 mM, the reaction rates remain the

DMSO and TFP Concentrations. DMSO is an excellent solvent to dissolve APIs with a wide range of polarity and is convenient for storage due to its low volatility and high stability. However, excess DMSO may be detrimental to the current method because DMSO can bind to palladium to form resting-state palladium species. Therefore, we hypothesized that tolerable DMSO concentrations might depend on the TFP concentration. To determine the optimum concentration range for these two components, we titrated them in a combinatorial manner (Figure 5c) to find that 5-10% DMSO and $100-220~\mu M$ TFP were acceptable.

Metal Selectivity and Interference. When a palladium-catalyzed reaction is employed, palladium is obviously the major concern with respect to metal contamination. However, other metal contaminations may be present because other reagents, glassware, or water used during purification may contain copper and iron, among other heavy metals. The previous method was fairly selective for palladium, but platinum produced approximately one-fifth of the signal compared to palladium. Figure 6a shows that the current method is more selective for palladium (41810 AU), with platinum (9242 AU) being second most reactive. More specifically, after the background (no metal; 5677 AU) subtraction, we determined that the selectivity between palladium and platinum was 10:1.

We then tested whether other metals would interfere with the quantification of palladium. In the presence of other metals at 345, 30 nM palladium was detected fairly accurately, with the exception of silver ions (Figure 6b,c). The reason for the interference is currently unknown. Given the aforementioned reactivity of platinum, it was not surprising that the mixture of 30 nM palladium and 345 nM platinum generated a stronger signal than 30 nM palladium alone. Therefore, in instances where both palladium- and platinum-catalyzed reactions are performed in the same synthetic sequence, it would be prudent that a more palladium-selective fluorometric method (manuscript in preparation) be employed. Also, if silver is suspected as a





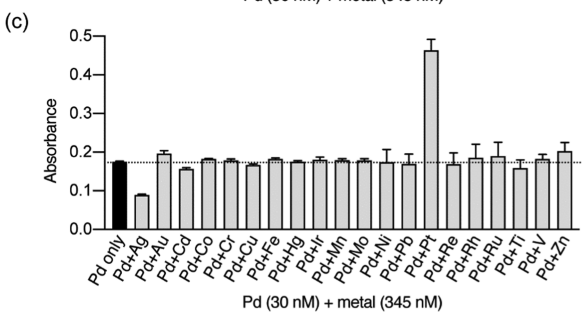


Figure 6. (a) Fluorescence values refer to emission signals in the 580–640 nm range with excitation at 525 nm. Metal selectivity. Conditions: 180 μM TFP, 30 μM RAE, 1.0 mM NaBH₄, 100 mM NaOH, 200 mM NH₄OAc, 5:17:78 v/v DMSO/H₂O/EtOH, Metal: no metal or 30 nM Ti, V, Cr, Mn, Fe, Co, Ni, Cu, Zn, Mo, Ru, Rh, Pd, Ag, Cd, Re, Ir, Pt, Au, Hg, Pb, 24 °C, 60 min, n=3. (b) Fluorescence values refer to emission signals in the 580–640 nm range with excitation at 525 nm. Metal interference. Conditions: 180 μM TFP, 30 μM RAE, 1.0 mM NaBH₄, 100 mM NaOH, 200 mM NH₄OAc, 5:17:78 v/v DMSO/H₂O/EtOH, Metal: 30 nM Pd and no metal or 345 nM Ti, V, Cr, Mn, Fe, Co, Ni, Cu, Zn, Mo, Ru, Rh, Pd, Ag, Cd, Re, Ir, Pt, Au, Hg, or Pb, 24 °C, 60 min, n=3. (c) UV—vis data of b at 560 nm.

contaminant in large excess relative to palladium, ICP-MS analysis for silver ions may be necessary.

Quantification. Synthetic samples prepared by palladium-catalyzed reactions may contain 10–2000 ppm palladium in the solid state. If 1 mg of synthetic material as the solid is dissolved in 1 mL liquid, the resulting palladium concentrations will be 10–2000 ppb. In the metal analysis, if an aliquot (20 μ L) is added to an assay solution (180 μ L), the resulting mixture will contain 1–200 ppb (9.4–1880 nM) palladium.

With this in mind, we examined the correlation between palladium concentrations and fluorescence intensities. First, with 180 μ M TFP, 30 μ M RAE, 1.0 mM NaBH₄, 200 mM NH₄OAc in 5:17:78 v/v DMSO/H₂O/EtOH, the reactions were carried out for 1 h in the 0–2000 nM palladium range (Figure 7a), revealing that the method was quantitative up to 250 nM. By lowering the NaBH₄ concentration from 1 to 0.5 mM, the dynamic range broadened, at the expense of sensitivity (Figure 7b). The sensitivity could be improved by

Organic Process Research & Development

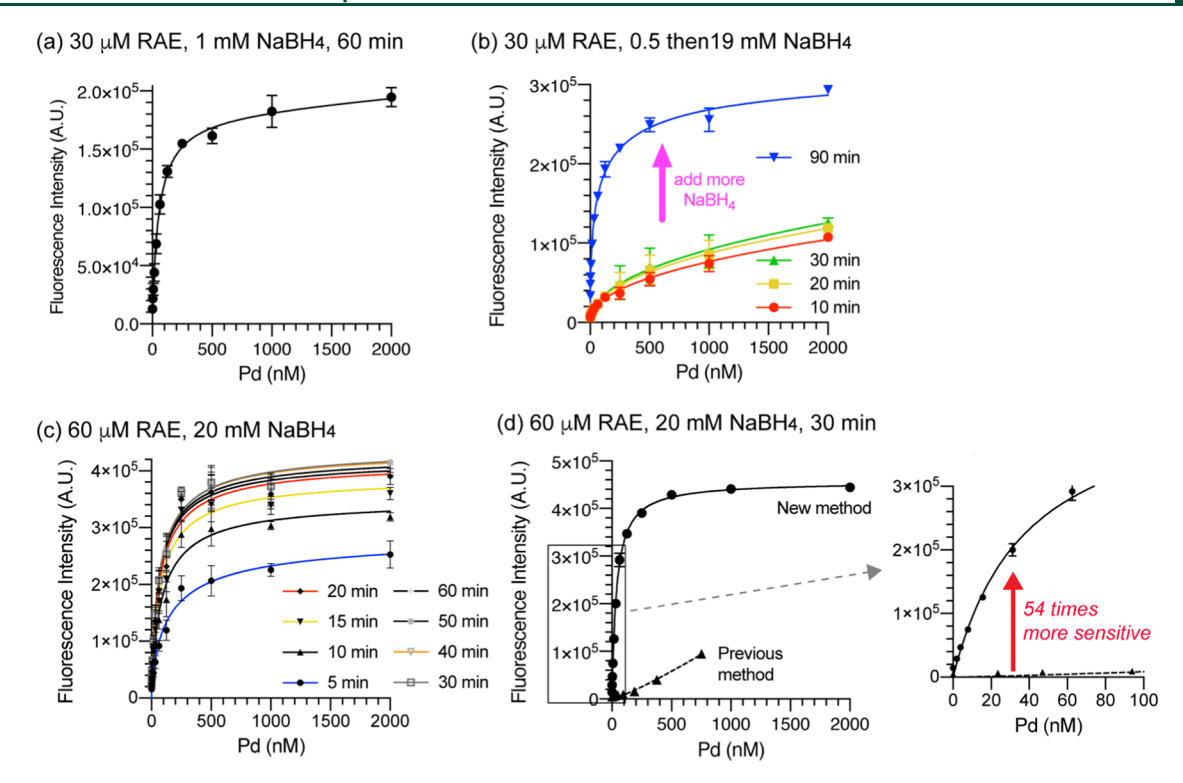


Figure 7. Correlation between palladium concentration (0–2000 nM) and fluorescence intensity. Fluorescence values refer to emission signals in the 580–640 nm range with excitation at 525 nm. Common conditions for the four graphs: 180 μ M TFP, 200 mM NH₄OAc, 5–9:17:78–74 v/v DMSO/H₂O/EtOH, 24 °C. Variables: (a) 30 μ M RAE, 1.0 mM NaBH₄, 100 mM NaOH, 24 °C, 1 h, n = 3. (b) 30 μ M RAE, 0.5 mM NaBH₄, 25 mM NaOH, 30 min, n = 4. Then add more NaBH₄. (c) 60 μ M RAE, 20 mM NaBH₄, 75 mM NaOH, 60 min, n = 3. (d) 60 μ M RAE, 20 mM NaBH₄, 75 mM NaOH, 30 min, n = 3.

the second addition of NaBH₄ (stop-and-go) to increase the NaBH₄ concentration to 19 mM. To omit the second addition of NaBH₄ for procedural simplicity, we started the reactions with 20 mM NaBH₄, with the expectation that the data at earlier points might be more linear because less substrate (RAE) would be consumed. However, even the 5 min data point showed a nonlinear trend (Figure 7c). These data were reproducible; Figure 7d shows the result under the same conditions on a different day. This figure also compares the current method with our previous method,²³ indicating that the current method is 54 times more sensitive in the 0–32 nM palladium concentration range.

We hypothesized that this reaction might follow Michaelis—Menten kinetics because there may be pre-equilibrium among palladium, TFP, and RAE to form the catalyst—substrate complex. To test this hypothesis, we measured the velocity as a function of substrate concentration (Figure 8). To slow the reaction to measure fluorescence intensities for the first several minutes accurately, we lowered the NaBH₄ concentration to 0.5 mM. Indeed, we observed the saturation kinetics, indicating that the palladium-catalyzed deallylation fits Michaelis—Menten kinetics.

Validation of the Method. The purpose of implementing a high-throughput screening method for palladium is not to accurately measure the absolute concentrations of palladium in APIs but to estimate the relative concentrations of palladium when process chemists screen for dozens of scavenging methods. One of the major challenges is to semiquantify palladium at as low as 10 ppm and as high as 2000 ppm. We must consider the solubility of APIs and stability of palladium when solutions of APIs are prepared for analysis. If an API

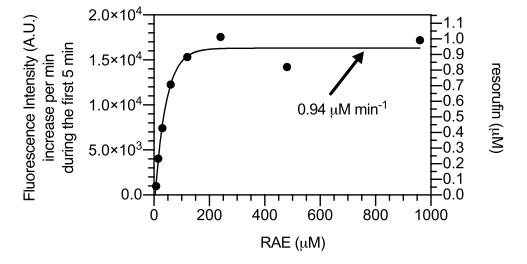


Figure 8. Saturation kinetics. Fluorescence values refer to emission signals in the 580–640 nm range with excitation at 525 nm. Conditions: 7.5–960 μ M RAE, 180 μ M TFP, 0.5 mM NaBH₄, 75 mM NaOH, 200 mM NH₄OAc, 8.7:17:74.3 v/v DMSO/H₂O/EtOH, 31 nM PdCl₂, 24 °C.

substance (1 mg) with X ppm palladium in the solid state is dissolved in 500 mM HCl in 1:4 DMSO/H₂O (1.0 mL), the resultant concentrations are 1 mg API/mL and X ppb (9.4X nM) palladium. When this solution (20 μ L) is added to a reaction mixture (180 μ L) in a well, the palladium concentration is 0.1X ppb (0.94X nM). Therefore, when the palladium concentration in the well is determined to be Y nM, the palladium content in the original solid API is Y/0.94 ppm.

To target the 0–250 nM palladium range in the assay solutions with various amounts of palladium in mock APIs, we chose to subject 1.0 and 0.1 mg/mL mock API solutions to the reaction conditions. In a double-blinded manner, a member in our research group, who was not part of this study, prepared solutions of drugs spiked with known amounts of palladium. Four or five days after the samples were prepared, we analyzed these samples in three separate experiments. We used freshly diluted palladium solutions with known concentrations to

create a calibration curve. The results are summarized in Table 2. On average, the error was 57%. An origin of error may stem

Table 2. Evaluation of the Current Method with Mock APIs

material ID	Pd (ppm) in solid determined by the current method	actual Pd (ppm) in solid	% error
6-bromoindole A	95	45	111
6-bromoindole B	85	405	79
6-bromoindole C	<1	0	
tyrosine A	19	15	27
tyrosine B	4	5	20
tyrosine C	73	45	62
shikimic acid A	10	15	33
shikimic acid B	209	405	48
shikimic acid C	871	1215	28
uridine A	<1	0	
uridine B	>2000	1215	
uridine C	96	45	113
biotin A	9	15	40
biotin B	225	405	44
biotin C	4	5	20
brucine A	<1	0	
brucine B	219	135	62
brucine C	53	45	18
yohimbine A	>2000	1215	
yohimbine B	116	135	14
yohimbine C	3	5	40
progesterone A	33	45	27
progesterone B	44	135	67
progesterone C	12	5	140
imatinib A	<1	5	
imatinib B	140	135	4
imatinib C	1210	405	199
average % error			57

from the age of the samples; we compared 4- to 5-day old palladium solutions with freshly prepared palladium standard solutions. Nonetheless, the graph shown in Figure 9 indicates that our method is an enabling technology to determine the relative concentrations of palladium.

Finally, we analyzed synthetic samples that were produced by palladium-catalyzed reactions in our laboratory for unrelated projects. The same stock solutions of these samples were also analyzed by ICP-MS as a reference. Table 3 and

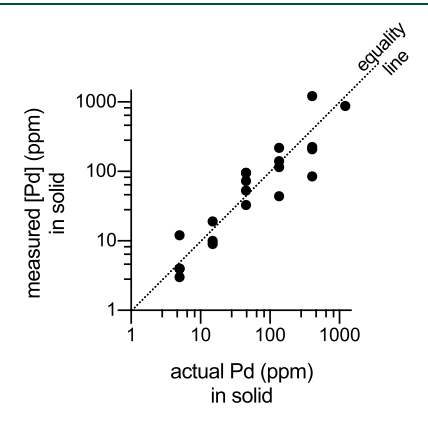


Figure 9. Correlation between ICP-MS and the current method with mock API samples.

Table 3. Comparison between the Current Method and ICP-MS Using Actual Synthetic Samples with Unknown Amounts of Palladium^a

sample ID	Pd (ppm) in solid measured by the current method	Pd (ppm) in solid measured by ICP-MS	% error
BMK1030	1149	600	92
RKB9101 crude	1306	648	102
RKB9101 after CC	438	365	20
RKB9102 impure	3293	3321	1
RKB9102 after resin	594	146	307
PLM3108A	3	<1	
PLM3108B	2	<1	
PLM3109A	1	1	0
PLM3109B	2	<1	
RKB9019	135	63	114
JAB7140	5808	9776	41
JAB7140 purified	175	237	26
JAB7141	9480	5979	59
JAB7141 purified	113	159	29
average % error			72

"The values were calculated for palladium concentrations in synthetic compounds in the solid state.

Figure 10 summarize the results. In general, the current method is not yet optimal for samples containing more than

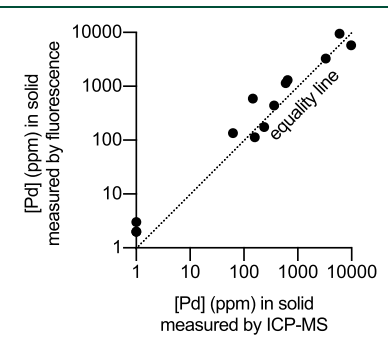


Figure 10. Correlation between ICP-MS and the current method with synthetic samples.

1000 ppm palladium. The plateaus we observed in Figure 7 are due to the full consumption of RAE (cf. Figure 1). We recommend that palladium-rich samples should be further diluted prior to analysis. Otherwise, the current method showed the correct trend for relative palladium concentrations. There were three samples (PLM3108A, PLM3108B, and PLM3109B) that must be contaminated with trace palladium because they were synthesized by Pd/C-catalyzed hydrogenation reactions. ICP-MS could not detect the metal, but the current method could. The average error (72%) was greater with synthetic samples than with mock samples (57%) because unlike spiked mock samples, the synthetic compounds may bind to palladium ions during long periods of storage. This hypothesis warrants further extensive studies in the future.

Scheme 2. Proposed Mechanism for the Reaction of RAE with NaOH

Scheme 3. (a) Typical Enzyme-Catalyzed Reactions with Michalis-Menten Kinetics; (b) Analogy of the Current Method to (a)

DISCUSSION

We set a goal of understanding how the multiple components in the fluorometric/colorimetric method may influence the outcome. The addition of NaOH was inevitable because NaBH₄ was essential for the palladium-catalyzed allylic C-O bond cleavage under air atmosphere, 23 and NaBH4 must be stabilized by NaOH in water. NaBH4 and NaOH react with NH₄OAc, and the resulting basicity influences the stability of NaBH₄. NH₄OAc was found to retard the reaction because it quenches NaBH4, but it was necessary to avoid acidic conditions in the assay. We titrated multiple components in a combinatorial manner for the first time since we began developing and applying fluorometric or colorimetric methods for palladium. ^{23,24,27,30,41–50} When there was more NaOH than NH₄OAc, the excess NaOH turned the solution purple in the absence of palladium. Although the UV-vis spectrum of the purple solution resembled that of resorufin, RAE was not converted to resorufin because neutralization with additional NH₄OAc or acid reversed the UV-vis spectrum back to that of RAE. The reversible reaction between RAE and NaOH was further supported by ¹H NMR analysis. Unfortunately, we were unable to determine the structure of the transient product under basic conditions due to its poor solubility in DMSO- d_{6} , CD₃OD, and D₂O. Based on the previously observed mode of reactivity of related resorufin derivatives,⁵¹ we speculate that NaOH undergoes reversible conjugate addition to form keto-1, which may be in equilibrium with its tautomer, enol-1 (Scheme 2).

Although the hypothesized mechanism may be intriguing, this is detrimental to achieving the goal of developing a palladium-specific quantification method. Thus, it is important to ensure that the NH₄OAc concentration exceeds the NaOH concentration. Our palladium stock solutions were stored in 500 mM HCl, which partially eliminated NaOH in assay solutions. Because of this background reaction identified in the current study, we changed the order of addition of reagents to avoid such an undesired reaction.

The stop-and-go strategy is convenient for those who have no access to continuous monitoring of the assay. For the current study, because we had access to an instrument that could read a 96-well plate every few minutes, we chose to opt for procedural simplicity. Figure 5b shows that the reaction rate (i.e., the sensitivity of the assay) can be fine-tuned by changing the NaBH₄ concentration. The optimum ranges of TFP and DMSO concentrations were 100–220 μ M and 5–10% v/v, respectively. Too much TFP slowed the reaction, presumably because TFP began to form coordinatively saturated (i.e., unreactive) palladium species in situ. DMSO can bind and form catalytically inactive palladium species, which is likely why more than 10% DMSO substantially retarded the reaction.

Although platinum showed reactivity under the reaction conditions, palladium was about 10 times more reactive. Only silver (12 equiv relative to palladium) showed significant interference, the molecular mechanism of which is currently unknown.

Achieving a broad dynamic range for any fluorometric or colorimetric method is a formidable challenge in chemistry and biology. For example, a commercial kit for hydrogen peroxide by fluorescence can be effective between 0.1 and 1 mM concentrations. Our method was quantitative in the 2–250 nM palladium concentration range. Therefore, if the palladium concentration in an API is expected to be above 250 ppm in the solid state, we recommend that the stock solutions of the sample should be diluted to 0.1 mg/mL or lower. Comparison of the current method and our previous method²³ revealed that the initial reaction rate is 54 times faster (i.e., the current method is 54 times more sensitive; Figure 7d).

We evaluated the current method with drugs or drug-like compounds spiked with known amounts of palladium. Possibly because the spiking was performed 4-5 days prior to the assays, the current method underestimated palladium concentrations in some instances. It is important to note that the method showed the expected relative concentrations of palladium, which may fulfill users' needs in high-throughput screenings of palladium scavenging to determine the relative efficiency of the scavengers. With 14 synthetic samples prepared by palladium-catalyzed reactions, we compared the current method with ICP-MS. In this case study, the average percent error value was slightly greater than that of the study with mock samples. Nonetheless, the relative concentrations of palladium boded well with ICP-MS. We believe that these results are remarkable, considering the fact that the samples were not digested. If we develop a protocol to fully restore the palladium reactivity under the reaction conditions through

Organic Process Research & Development

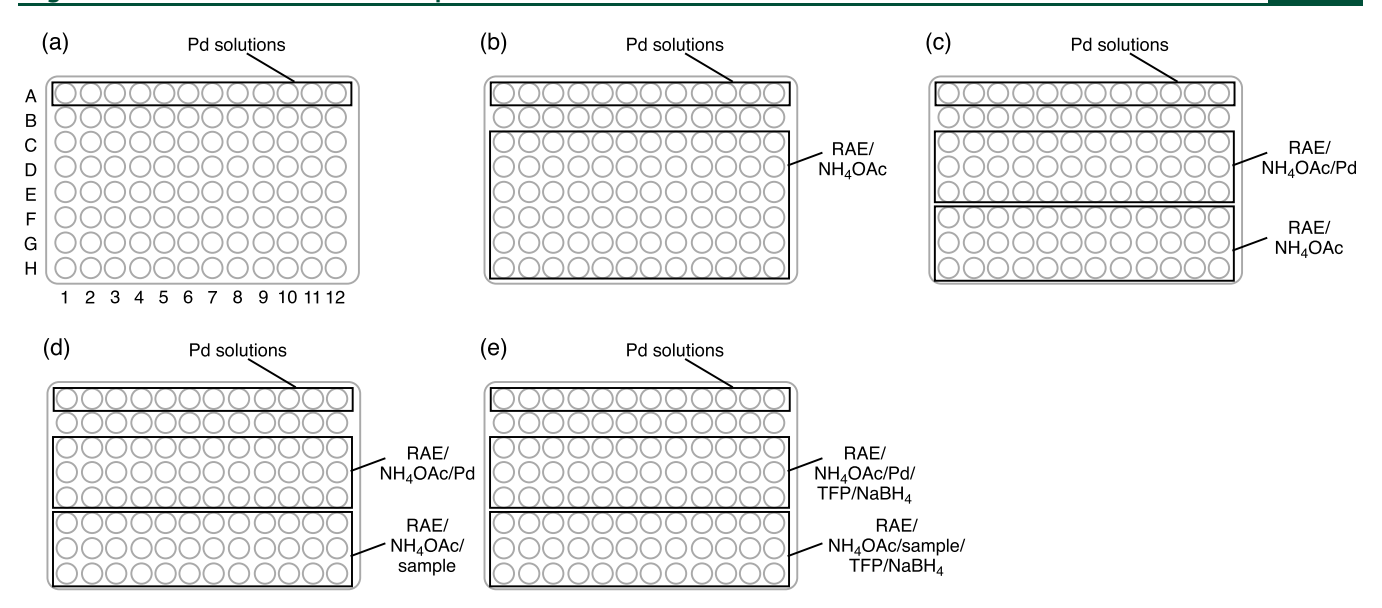


Figure 11. Plate map for the assay.

digestion (e.g., microwave digestion⁵²), the accuracy may be further improved.

Finally, we discovered that the palladium-catalyzed Tsuji—Trost reaction under the current reaction conditions fit Michaelis—Menten kinetics. Michaelis—Menten kinetics in transition-metal-catalyzed reactions were discussed in the literature, although scarcely. This is surprising since Pirrung and co-workers stated that there might be many such reactions. He saturation kinetics experiment depicted in Figure 8 shows that increasing the RAE concentration up to $\sim 120~\mu$ M will linearly increase the reaction rate. Scheme 3a (general equation for Michaelis—Menten kinetics) can be applied to Scheme 3b, in which the π -allylpalladium complex is equivalent to an enzyme—substrate complex depicted in the original paper by Michaelis and Menten. S6,57

CONCLUSIONS

We developed a robust method with lower background signals to semiquantify palladium at nanomolar concentrations. The method may prove to be useful for real-world samples. We also discovered that the reaction follows Michaelis—Menten kinetics.

Representative Experimental Procedure. *Preparation of 0.5 M HCl in 1:4 v/v DMSO/Water (Solution B).* DMSO (10.0 mL) and 625 mM HCl in water (40.0 mL) were mixed in an amber glass bottle.

Preparation of 85.7 μ M RAE/286 mM NH₄OAc in 10.7:89.3 v/v DMSO/EtOH. RAE (25.3 mg) was dissolved in DMSO (20.00 mL) in an amber vial to prepare 5.0 mM RAE in DMSO. Subsequently, an aliquot of this solution (8.0 mL) was diluted with EtOH (42.0 mL) in an amber bottle to prepare an 800 μ M RAE in 4:21 v/v DMSO/EtOH solution. The 800 μ M RAE solution in DMSO (32.14 mL) was mixed with 500 mM NH₄OAc (171.6 mL) and EtOH (96.26 mL) in a 500-mL amber bottle. All of the solutions were stored at -20 °C.

Preparation of 0, 19.6, 39.1, 78.1, 156, 313, 625, 1250, 2500, 5000, 10 000, and 20 000 nM Pd Solutions. A 1000 ppm (9.4 mM) palladium standard solution in 10% w/v HCl (2.7 M HCl) for atomic absorption spectroscopy was purchased from Fisher and stored at 24 °C. This solution (240 μ L) was diluted with 0.7 M trace metal HCl in water

(896 μ L) to prepare a 2.0 mM Pd solution (1.136 mL). This solution can be stored at 24 °C for at least 3 months. An aliquot of the 2.0 mM Pd solution (100 μ L) was diluted with solution B (900 μ L) to prepare 200 μ M Pd. A portion of this resulting solution (100 μ L) was diluted with solution B (900 μL) in row H, column 12 of a deep 96-well plate to prepare 20 μ M Pd. Solution B (500 μ L per well) was added to row H, columns 1-11 of a deep 96-well plate (1 mL per well). A 2fold serial dilution was performed in the deep 96-well plate until 19.6 nM Pd was prepared in column 2, row H. In each dilution step, the solutions were mixed thoroughly. Solution B (500 μ L; Pd-free) was added to column 1, row H. With an 8or 12-channel pipette, an aliquot of each Pd or Pd-free solution (150 μ L) was transferred to row A columns 1–12 of a black 96-well plate with a clear bottom (Figure 11a). We recommend that Pd solutions below 2 mM should be used within 6 h.

Preparation of Synthetic Samples in Solution **B** (1.0 and 0.05 mg/mL). Solid synthetic samples were dissolved in DMSO to prepare 5.0 mg/mL solutions. An aliquot of each solution (20 μ L) was diluted with 625 mM HCl (80 μ L) to prepare 1.0 mg/mL in a black 96-well plate. An aliquot of each of these solutions (5.0 μ L) was diluted with solution **B** (95 μ L) to prepare 0.05 mg/mL solutions.

Preparation of 900 μ M TFP/100 mM NaBH₄/375 mM NaOH in 6:44:50 v/v DMSO/EtOH/Water. One NaBH₄ pellet (1.00 g; 26.4 mmol) was dissolved in cold aqueous 10 M NaOH (9.91 mL) to prepare 2.67 M NaBH₄ and 10 M NaOH in water, which was kept on ice for up to 8 h. We recommend that this solution should be prepared within 8 h prior to use. CAUTION: Do not store the solution in a refrigerator due to the evolution of hydrogen gas.

Separately, butylated hydroxytoluene (BHT; 12.5 mg) was dissolved in DMSO (50 mL) in an amber bottle to prepare 250 ppm BHT in DMSO. The BHT solution in DMSO (6.667 mL) was used to dissolve TFP (23.2 mg; 100 μ mol) in an amber bottle to prepare 15.0 mM TFP in DMSO. This solution could be stored at 24 °C for at least 6 months.

Immediately after palladium-containing solutions were added in the assay, a solution of $2.67~M~NaBH_4$ and 10~M~NaOH in water (1.80~mL) was diluted with water (10.20~mL)

in a 15-mL conical centrifuge tube to prepare 400 mM NaBH₄ and 1.5 M NaOH in water. Subsequently, this solution (3.00 mL), cold EtOH (5.28 mL), 15.0 mM TFP in DMSO (720 μ L), and water (3.00 mL) were mixed in a reservoir to prepare 900 μ M TFP/100 mM NaBH₄/375 mM NaOH in 6:44:50 v/v DMSO/EtOH/water (12.00 mL).

Final Assay Conditions in Wells. 180 μ M TFP, 60 μ M RAE, 20 mM NaBH₄, 75 mM NaOH, 200 mM NH₄OAc, 8.7:17.0:74.3 v/v DMSO/water/EtOH, 0–2000 nM Pd, total volume = 200 μ L, 24 °C, 30 min, n = 3.

With an 8- or 12-channel pipette, the solution of 85.7 μ M RAE/286 mM NH₄OAc in 10.7:89.3 v/v DMSO/EtOH (140 μ L per well) was transferred from the reservoir to rows C–H, columns 1–12 on the black 96-well plate with a clear bottom (Figure 11b).

With an 8- or 12-channel pipette, 0, 19.6, 39.1, 78.1, 156, 313, 625, 1250, 2500, 5000, 10 000, and 20 000 nM Pd (20 μ L) were transferred from row A to rows C–E of the plate (triplicate; Figure 11c).

With an 8- or 12-channel pipette, 1.0 and 0.05 mg/mL synthetic samples (20 μ L) were transferred to rows F–H, columns 1–12 of the plate (triplicate; Figure 11d).

With an 8- or 12-channel pipette, the solution of 900 μ M TFP/100 mM NaBH₄/375 mM NaOH in 6:44:50 v/v DMSO/EtOH/water (40 μ L per well) was transferred from the reservoir to rows C–H, columns 1–12.

Absorbance signals (560 nm) or fluorescence signals (excitation 525 nm, emission 580–640 nm) were measured after 30 min. All fluorescence measurements (excitation 525 nm, emission 580–640 nm) in this study were carried out using a Promega Biosystems Modulus II Microplate Reader.

Data Analysis. Signals would be a function of palladium concentration. For unknown samples, palladium concentrations could be determined by the signal intensities.

■ ASSOCIATED CONTENT

S Supporting Information

The Supporting Information is available free of charge at https://pubs.acs.org/doi/10.1021/acs.oprd.9b00472.

Experimental procedures; instrumentation; reagents; general procedures; preparation of stock solutions; raw data for Table 1 and Figure 2a (fluorescence of resorufin as a function of palladium concentration at 16 min) (Table S1) (PDF)

AUTHOR INFORMATION

Corresponding Author

*E-mail: koide@pitt.edu.

ORCID

Kazunori Koide: 0000-0001-8894-8485

Notes

The authors declare no competing financial interest.

■ ACKNOWLEDGMENTS

L.L. is a recipient of the Summer Undergraduate Research Fellowship from the Chemistry Department of the University of Pittsburgh. This work was supported by the US National Science Foundation (CHE-1506942).

■ REFERENCES

(1) Pohl, P.; Bielawska-Pohl, A.; Dzimitrowicz, A.; Jamroz, P.; Welna, M. Impact and practicability of recently introduced require-

- ments on elemental impurities. TrAC, Trends Anal. Chem. 2018, 101, 43-55.
- (2) Boström, J.; Brown, D. G.; Young, R. J.; Keserü, G. M. Expanding the medicinal chemistry synthetic toolbox. *Nat. Rev. Drug Discovery* **2018**, *17*, 709–727.
- (3) Reginato, G.; Sadler, P.; Wilkes, R. D. Scaling up metal scavenging operations for pharmaceutical pilot plant manufactures. *Org. Process Res. Dev.* **2011**, *15*, 1396–1405.
- (4) Wang, L.; Green, L.; Li, Z.; McCabe Dunn, J.; Bu, X.; Welch, C. J.; Li, C.; Wang, T.; Tu, Q.; Bekos, E.; Richardson, D.; Eckert, J.; Cui, J. Screening binary systems of chelating agents combined with carbon or silica gel adsorbents: The development of a cost-effective method to remove palladium from pharmaceutical intermediates and APIs. Org. Process Res. Dev. 2011, 15, 1371–1376.
- (5) Magano, J. Large-scale Applications of Transition Metal Removal Techniques in the Manufacture of Pharmaceuticals. In *Transition Metal-Catalyzed Couplings in Process Chemistry: Case Studies from the Pharmaceutical Industry;* Magano, J., Dunetz, J. R., Eds.; Wiley-VCH Verlag GmbH & Co: KGaA, 2013; pp 313–355.
- (6) Mondal, B.; Wilkes, R. D.; Percy, J. M.; Tuttle, T.; Black, R. J. G.; North, C. Towards a quantitative understanding of palladium metal scavenger performance: an electronic structure calculation approach. *Dalton Trans.* **2014**, 43, 469–478.
- (7) Miyamoto, H.; Sakumoto, C.; Takekoshi, E.; Maeda, Y.; Hiramoto, N.; Itoh, T.; Kato, Y. Effective method to remove metal elements from pharmaceutical intermediates with polychelated resin scavenger. *Org. Process Res. Dev.* **2015**, *19*, 1054–1061.
- (8) Phillips, S.; Holdsworth, D.; Kauppinen, P.; Namara, C. M. Palladium impurity removal from active pharmaceutical ingredient process streams. *Johnson Matthey Technol. Rev.* **2016**, *60*, 277–286.
- (9) Yamada, T.; Matsuo, T.; Ogawa, A.; Ichikawa, T.; Kobayashi, Y.; Masuda, H.; Miyamoto, R.; Bai, H. Z.; Meguro, K.; Sawama, Y.; Monguchi, Y.; Sajiki, H. Application of thiol-modified dual-pore silica beads as a practical scavenger of leached palladium catalyst in C-C coupling reactions. *Org. Process Res. Dev.* **2019**, 23, 462–469.
- (10) Phillips, S.; Holdsworth, D.; Kauppinen, P.; Mac Namara, C. Palladium impurity removal from active pharmaceutical ingredient process streams. *Johnson Matthey Technol. Rev.* **2016**, *60*, 277–286.
- (11) Yamada, T.; Kobayashi, Y.; Ito, N.; Ichikawa, T.; Park, K.; Kunishima, K.; Ueda, S.; Mizuno, M.; Adachi, T.; Sawama, Y.; Monguchi, Y.; Sajiki, H. Polyethyleneimine-modified polymer as an efficient palladium scavenger and effective catalyst support for a functional heterogeneous palladium catalyst. ACS Omega 2019, 4, 10243–10251.
- (12) Cao, J.; Xu, G.; Xie, Y.; Tao, M.; Zhang, W. Thiourea modified polyacrylnitrile fibers as efficient Pd(II) scavengers. *RSC Adv.* **2016**, *6*, 58088–58098.
- (13) Gallagher, W. P.; Vo, A. Dithiocarbamates: Reagents for the removal of transition metals from organic reaction media. *Org. Process Res. Dev.* **2015**, *19*, 1369–1373.
- (14) Waller, D.; Gazda, G.; Minden, Z.; Barton, L.; Leigh, C. Synthesis of cephalosporin compounds. WO Patent WO2016/0258392016.
- (15) Ren, H.; Strulson, C. A.; Humphrey, G.; Xiang, R.; Li, G. T.; Gauthier, D. R.; Maloney, K. M. Potassium isopropyl xanthate (PIX): an ultra-efficient palladium scavenger. *Green Chem.* **2017**, *19*, 4002–4006
- (16) Olesik, J. W. Elemental analysis using ICP-OES and ICP/MS an evaluation and assessment of remaining problems. *Anal. Chem.* **1991**, *63*, 12A–21A.
- (17) Lewen, N.; Mathew, S.; Schenkenberger, M.; Raglione, T. A rapid ICP-MS screen for heavy metals in pharmaceutical compounds. *J. Pharm. Biomed. Anal.* **2004**, *35*, 739–752.
- (18) Rao, R. N.; Talluri, M. V. N. K. An overview of recent applications of inductively coupled plasma-mass spectrometry (ICP-MS) in determination of inorganic impurities in drugs and pharmaceuticals. *J. Pharm. Biomed. Anal.* **2007**, *43*, 1–13.
- (19) Al-Ammar, A. S.; Northington, J. Accuracy improvement in the determination of palladium in pharmaceuticals by eliminating

- volatility error when using ICP-MS coupled with direct introduction of sample dissolved in organic solvents. *J. Anal. At. Spectrom.* **2011**, *26*, 1531–1533.
- (20) Pluháček, T.; Rucka, M.; Maier, V. A direct LA-ICP-MS screening of elemental impurities in pharmaceutical products in compliance with USP and ICH-Q3D. *Anal. Chim. Acta* **2019**, *1078*, 1–7.
- (21) Tu, S.; Yusuf, S.; Muehlfeld, M.; Bauman, R.; Vanchura, B. The destiny of palladium: Development of efficient palladium analysis techniques in enhancing palladium recovery. *Org. Process Res. Dev.* **2019**, 23, 2175–2180.
- (22) Welch, C. J. High throughput analysis enables high throughput experimentation in pharmaceutical process research. *React. Chem. Eng.* **2019**, *4*, No. 1895.
- (23) Koide, K.; Tracey, M. P.; Bu, X.; Jo, J.; Williams, M. J.; Welch, C. J. A competitive and reversible deactivation approach to catalysis-based quantitative assays. *Nat. Commun.* **2016**, *7*, No. 10691.
- (24) Bu, X.; Williams, M.; Jo, J.; Koide, K.; Welch, C. J. Online sensing of palladium in flowing streams. *Chem. Commun.* **2017**, *53*, 720–723.
- (25) Andersen, N. G.; Keay, B. A. 2-Furyl phosphines as ligands for transition-metal-mediated organic synthesis. *Chem. Rev.* **2001**, *101*, 997–1030.
- (26) Farina, V.; Krishnan, B. Large rate accelerations in the Stille reaction with tri-2-furylphosphine and triphenylarsine as palladium ligands: Mechanistic and synthetic implications. *J. Am. Chem. Soc.* **1991**, *113*, 9585–9595.
- (27) Garner, A. L.; Song, F. L.; Koide, K. Enhancement of a catalysis-based fluorometric detection method for palladium through rational fine-tuning of the palladium species. *J. Am. Chem. Soc.* **2009**, 131, 5163–5171.
- (28) Pohorilets, I.; Tracey, M. P.; LeClaire, M. J.; Moore, E. M.; Lu, G.; Liu, P.; Koide, K. Kinetics and inverse temperature dependence of a Tsuji—Trost reaction in aqueous buffer. *ACS Catal.* **2019**, 11720—11733.
- (29) Balamurugan, R.; Liu, J. H.; Liu, B. T. A review of recent developments in fluorescent sensors for the selective detection of palladium ions. *Coord. Chem. Rev.* **2018**, *376*, 196–224.
- (30) Tracey, M. P.; Pham, D.; Koide, K. Fluorometric imaging methods for palladium and platinum and the use of palladium for imaging biomolecules. *Chem. Soc. Rev.* **2015**, *44*, 4769–4791.
- (31) Miller, M. A.; Askevold, B.; Mikula, H.; Kohler, R. H.; Pirovich, D.; Weissleder, R. Nano-palladium is a cellular catalyst for in vivo chemistry. *Nat. Commun.* **2017**, *8*, No. 15906.
- (32) Martínez-Calvo, M.; Couceiro, J. R.; Destito, P.; Rodríguez, J.; Mosquera, J.; Mascareñas, J. L. Intracellular deprotection r eactions mediated by palladium complexes equipped with designed phosphine ligands. ACS Catal. 2018, 6055–6061.
- (33) Ohana, R. F.; Levin, S.; Wood, M. G.; Zimmerman, K.; Dart, M. L.; Schwinn, M. K.; Kirkland, T. A.; Hurst, R.; Uyeda, H. T.; Encell, L. P.; Wood, K. V. Improved deconvolution of protein targets for bioactive compounds using a palladium cleavable chloroalkane capture tag. ACS Chem. Biol. 2016, 11, 2608–2617.
- (34) Yusop, R. M.; Unciti-Broceta, A.; Johansson, E. M. V.; Sanchez-Martin, R. M.; Bradley, M. Palladium-mediated intracellular chemistry. *Nat. Chem.* **2011**, *3*, 239–243.
- (35) Chankeshwara, S. V.; Indrigo, E.; Bradley, M. Palladium-mediated chemistry in living cells. *Curr. Opin. Chem. Biol.* **2014**, *21*, 128–135.
- (36) Li, J.; Yu, J. T.; Zhao, J. Y.; Wang, J.; Zheng, S. Q.; Lin, S. X.; Chen, L.; Yang, M. Y.; Jia, S.; Zhang, X. Y.; Chen, P. R. Palladium-triggered deprotection chemistry for protein activation in living cells. *Nat. Chem.* **2014**, *6*, 352–361.
- (37) Weiss, J. T.; Dawson, J. C.; Fraser, C.; Rybski, W.; Torres-Sanchez, C.; Bradley, M.; Patton, E. E.; Carragher, N. O.; Unciti-Broceta, A. Development and bioorthogonal activation of palladium-labile prodrugs of gencitabine. *J. Med. Chem.* **2014**, *57*, 5395–5404.
- (38) Weiss, J. T.; Dawson, J. C.; Macleod, K. G.; Rybski, W.; Fraser, C.; Torres-Sánchez, C.; Patton, E. E.; Bradley, M.; Carragher, N. O.;

- Unciti-Broceta, A. Extracellular palladium-catalysed dealkylation of 5-fluoro-1-propargyl-uracil as a bioorthogonally activated prodrug approach. *Nat. Commun.* **2014**, *5*, No. 3277.
- (39) Biswas, S.; McCullough, B. S.; Ma, E. S.; LaJoie, D.; Russell, C. W.; Brown, D. G.; Round, J. L.; Ullman, K. S.; Mulvey, M. A.; Barrios, A. M. Dual colorimetric and fluorogenic probes for visualizing tyrosine phosphatase activity. *Chem. Commun.* **2017**, *53*, 2233–2236.
- (40) Lyttle, D. A.; Jensen, E. H.; Struck, W. A. A simple volumetric assay for sodium borohydride. *Anal. Chem.* **1952**, *24*, 1843–1844.
- (41) Song, F. L.; Carder, E. J.; Kohler, C. C.; Koide, K. Studies toward an ideal fluorescence method to measure palladium in functionalized organic molecules: effects of sodium borohydride, temperature, phosphine ligand, and phosphate ions on kinetics. *Chem. Eur. J.* **2010**, *16*, 13500–13508.
- (42) Song, F. L.; Garner, A. L.; Koide, K. A highly sensitive fluorescent sensor for palladium based on the allylic oxidative insertion mechanism. *J. Am. Chem. Soc.* **2007**, *129*, 12354–12355.
- (43) Garner, A. L.; Koide, K. Oxidation state-specific fluorescent method for palladium(II) and platinum(IV) based on the catalyzed aromatic Claisen rearrangement. *J. Am. Chem. Soc.* **2008**, *130*, 16472–16473.
- (44) Garner, A. L.; Koide, K. Studies of a fluorogenic probe for palladium and platinum leading to a palladium-specific detection method. *Chem. Commun.* **2009**, 86–88.
- (45) Inamoto, K.; Campbell, L. D.; Doi, T.; Koide, K. A highly sensitive fluorescence method reveals the presence of palladium in a cross-coupling reaction mixture not treated with transition metals. *Tetrahedron Lett.* **2012**, *53*, 3147–3148.
- (46) Li, D.; Campbell, L. D.; Austin, B. A.; Koide, K. Detection of trace palladium in flasks and metal reagents using a fluorogenic Tsuji-Trost reaction. *ChemPlusChem* **2012**, *77*, 281–283.
- (47) Bu, X. D.; Koide, K.; Carder, E. J.; Welch, C. J. Rapid analysis of residual palladium in pharmaceutical development using a catalysis-based fluorometric method. *Org. Process Res. Dev.* **2013**, *17*, 108–113.
- (48) Williams, J. M.; Koide, K. A high-throughput method to detect palladium in ores. *Ind. Eng. Chem. Res.* **2013**, *52*, 8612–8615.
- (49) Koide, K. Palladium Detection Techniques for Active Pharmaceutical Ingredients Prepared via Cross-Couplings. In *New Trends in Cross-Coupling: Theory and Applications*; Colacot, T. J., Ed.; Royal Society of Chemistry, 2015.
- (50) Nieberding, M.; Tracey, M. P.; Koide, K. Noneffervescent method for catalysis-based palladium detection with color or fluorescence. *ACS Sens.* **2017**, *2*, 1737–1743.
- (51) Kitson, T. M. The oxidative addition reaction between compounds of resorufin (7-hydroxy-3*H*-phenoxazin-3-one) and 2-mercaptoethanol. *Bioorg. Chem.* **1998**, *26*, 63–73.
- (52) Pinheiro, F. C.; Barros, A. I.; Nobrega, J. A. Microwave-assisted sample preparation of medicines for determination of elemental impurities in compliance with United States Pharmacopeia: How simple can it be? *Anal. Chim. Acta* **2019**, *1065*, 1–11.
- (53) Corey, E. J.; Noe, M. C. Kinetic investigations provide additional evidence that an enzyme-like binding pocket is crucial for high enantioselectivity in the bis-cinchona alkaloid catalyzed asymmetric dihydroxylation of olefins. *J. Am. Chem. Soc.* **1996**, *118*, 319–329.
- (54) Pirrung, M. C.; Liu, H.; Morehead, J. A. T. Rhodium chemzymes: Michaelis—Menten kinetics in dirhodium(II) carboxylate-catalyzed carbenoid reactions. *J. Am. Chem. Soc.* **2002**, *124*, 1014—1023.
- (55) Joshi, A. M.; MacFarlane, K. S.; James, B. R. Kinetics and mechanism of H_2 hydrogenation of styrene catalyzed by [RuCl-(dppb)(μ -Cl)]₂ (dppb = 1,4-bis(diphenylphosphino)butane). Evidence for hydrogen transfer from a dinuclear molecular hydrogen species. *J. Organomet. Chem.* **1995**, 488, 161–167.
- (56) Michaelis, L.; Menten, M. L. Die Kinetik der Invertinwirkung. *Biochem. Z.* 1913, 49, 333–369.
- (57) Johnson, K. A.; Goody, R. S. The original Michaelis constant: Translation of the 1913 Michaelis—Menten paper. *Biochemistry* **2011**, 50, 8264–8269.